LANGMUIR

pubs.acs.org/Langmuir Article

Benchmarks of SMA-Copolymer Derivatives and Nanodisc Integrity

Giacomo M. Di Mauro,* Carmelo La Rosa, Marcello Condorelli, and Ayyalusamy Ramamoorthy*

Cite This: *Langmuir* 2021, 37, 3113–3121 Read Online

ACCESS | Metrics & More | Article Recommendations | Supporting Information

ABSTRACT: Poly(styrene-*co*-maleic acid) or SMA and its derivatives, a family of synthetic amphipathic copolymers, are increasingly used to directly solubilize cell membranes to functionally reconstitute membrane proteins in native-like copolymer–lipid nanodiscs. Although these copolymers act, de facto, like a "macromolecular detergent", the polymer-based lipid-nanodiscs has been demonstrated to be an excellent membrane mimetic for structural and functional studies of membrane proteins and their complexes by a variety of biophysical and biochemical approaches. In many studies reported in the literature, the choice of the right SMA formulation can depend on a number of factors, and the experimental conditions are typically developed according to a trial-and-error process since each studied system requires adapted protocols. While increasing number of nanodisc-forming copolymers are reported to be useful and they provide flexibilities in optimizing the sample preparation conditions, it is important to develop a systematic protocol that can be used for various applications. In this context, there is a vital necessity of benchmarking the performances of existing copolymer formulations, assessing crucial parameters for the successful extraction, isolation, and stabilization of membrane proteins. In this study, we compare both copolymers and copolymer–lipid nanodiscs obtained by SMA-EA with a set of anionic XIRAN copolymer formulations commercially available under the names of SL25010 P, SL30010 P, and SL40005 P. The reported results show how the critical micellar concentration (c.m.c.) of each copolymer is significantly altered in the presence of lipids and confirms the existence of an equilibrium between nanodisc-bound and "free" or "micellar" copolymer chains in the solution. We believe that these findings can be exploited to optimize studies that involve the necessity of special copolymers, which would not only simplify the applications but also broaden the scope of polymer-based nanodiscs.

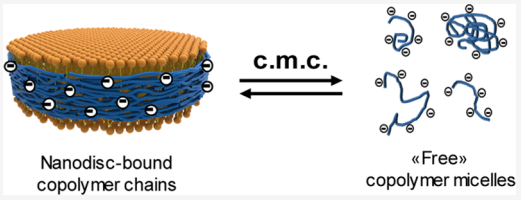

Downloaded via UNIV OF ALBERTA on June 1, 2022 at 21:19:58 (UTC).
See https://pubs.acs.org/sharingguidelines for options on how to legitimately share published articles.

Membrane proteins, essential components of any cellular membrane, are involved in many of the crucial cellular functions required for life and represent ∼60% of all drug targets.[1] However, despite the recent success in obtaining high-resolution structures,[2−5] our current understanding of cellular membrane biology and the development of modern drugs is hindered by the lack of structural information tied to the challenges in the extraction, isolation, and purification of functioning membrane proteins from their native cellular environment.[6−13] Poly(styrene-*co*-maleic acid), or SMA, is an amphipathic copolymer used to directly solubilize cell membranes and stabilize membrane proteins in nativelike discoidal copolymer–lipid nanoparticles, and it is composed of a lipid bilayer patch wrapped in a belt of amphipathic copolymer chains.[8−10,14−20] Acting, de facto, as a "macromolecular detergent", among its advantages, the SMA copolymer allows membrane proteins to retain lipids that are useful for both structural and functional purposes,[2−4,10,21−27] showing no preferences in the extraction.[28]

The SMA copolymer, however, is a generic denomination that identifies a variety of different formulations (SMAs); in fact, it can be readily customized.[29−34] For example, varying the molecular weight or the styrene-to-maleic acid ratio, it is possible to fine-tune the amphipathic properties and so as the ability of membrane solubilization.[35] Additionally, SMA copolymers can be further functionalized, expanding their range of applications.[11,17,19,36−40] Each formulation has both advantages and limitations that affect its applicability.[41] Indeed, the adoption of a suitable formulation is mostly connected to convenience and a trial-and-error process, since each studied system requires adapted protocols.[42]

Due to their amphipathic nature, SMAs exist mainly as individual copolymer chains in dilute solutions, while at high concentrations, they form a plethora of intra- and interchain copolymer micelles.[43] Such a variety is a result of intermolecular interactions, modulated by the balance between the hydrophobic effect and electrostatic repulsions, and is affected by the dispersity ($Đ$) of the copolymers.[35] Many parameters, such as the molecular weight (MW), the styrene-to-maleic acid ratio (x/y), and $Đ$, are currently used to assess SMA formulations. Additionally, as a polymeric "detergent", SMAs can be evaluated using parameters such as the critical micellar concentration (c.m.c.).[44]

Received: December 15, 2020
Revised: February 1, 2021
Published: March 1, 2021

© 2021 American Chemical Society

https://dx.doi.org/10.1021/acs.langmuir.0c03554
Langmuir 2021, 37, 3113–3121

Despite its definition, c.m.c. does not correspond to a single well-defined value. Still, it coincides with a range of concentrations and involves dynamic, association−dissociation equilibrium.[43,45] In the case of amphiphilic copolymers, their dispersity complicates the scenario. Indeed, the presence of chains of a variety of molecular weights[29] leads to distribution of aggregates of different sizes, both intra- and interchains. There have been many attempts to decrease the intrinsic dispersity of the copolymers by purification steps or finding alternative synthetic paths, but studies suggest that SMA's solubilization efficiency is connected to the variation of molecular weights.[33,43]

Copolymer−lipid nanodiscs are functional hybrid materials that arise from the synergistic interactions between two self-assembling materials, copolymers and phospholipids. For this reason, it is misleading to refer to both copolymer and phospholipids as individual entities. Indeed, once mixed, copolymers interact with phospholipids forming either nanodiscs or other randomly unstructured aggregates.

The necessity of benchmarking the performances of existing copolymers, assessing crucial parameters for the successful extraction and stabilization of membrane proteins, is compulsory for the advancement of the field. To facilitate the choice among the copolymer formulations commercially available, to assist the design of new alternatives, and to shed light on the behavior of copolymer−lipid nanodiscs, herein we compare a set of anionic SMAs. XIRAN SL25010 P, SL30010 P, and SL40005 P formulations (gift from Polyscience (Geleen, Netherlands)) were chosen because of their wide diffusion and success rate and compared to SMA-EA, a copolymer developed in our laboratory.[36] Each copolymer exhibits a different molecular weight, hydrophobic−hydrophilic ratio, and charge density, covering a wide range of features.

EXPERIMENTAL SECTION

Materials. 1,2-Dimyristoyl-*sn*-glycero-3-phosphocholine (DMPC) was purchased from Avanti Polar Lipids, Inc. (Alabaster, Alabama). Hydrochloric acid (HCl), sodium hydroxide (NaOH), ammonium acetate ($C_2H_7NO_2$), potassium phosphate monobasic (KH_2PO_4), potassium phosphate dibasic (K_2HPO_4), pyrene ($C_{16}H_{10}$), and sodium cholate hydrate ($C_{24}H_{39}NaO_5$) were purchased from Sigma-Aldrich (St. Louis, Missouri). SMA-EA was synthesized, purified, and characterized according to the procedure described in the literature. XIRAN SL25010 P, XIRAN SL30010 P, and XIRAN SL40005 P were kindly gifted by Polyscience (Geleen, Netherlands).

Methods. *Copolymer−Lipid Nanodisc Preparation.* A 20 mg/mL stock solution of each copolymer was prepared by weighing the copolymer powder and dissolving it in 0.1 M NaOH. After complete solubilization, the solution was neutralized by adding 1 M HCl dropwise, reaching a final pH 7.00. Copolymer-based lipid nanodiscs were obtained by mixing DMPC and copolymers in a 1:1 weight ratio (w/w). Each sample was then diluted to the desired final volume and incubated overnight at room temperature. SMA-EA, SL25010 P, and SL30010 P copolymer solution samples for the pyrene assay were prepared at an initial concentration of 2 mg/mL. For the SL40005 P solution, due to the high hydrophilicity of this copolymer, the starting concentration was 25 mg/mL. Copolymer−lipid nanodiscs were purified by size exclusion chromatography (SEC). For each copolymer formulation, 10 mg of lipids and 10 mg of copolymers were mixed, as explained previously, using 10 mM phosphate buffer at pH 7.2 and eluted at room temperature. All of the aliquots, associated with the nanodiscs' peak, were collected and mixed. This homogeneous solution was then divided into four aliquots of equal volume. Three of them were then used to perform the pyrene assay, while one was used for quantification using NMR experiments.

Preparation of the Pyrene-Buffer Stock Solution. A stock solution was prepared by solubilizing a known amount of pyrene in ethanol (95% v/v). A 1 μM water-based solution of pyrene was then prepared from its dilution with 10 mM ammonium acetate buffer (pH 7 at 25 °C). The study of purified nanodiscs was performed using 10 mM potassium phosphate buffer (pH 7 at 25 °C) to avoid spectral interferences with ^{1}H NMR. The ethanol content in the experimental solution was considered negligible and, as reported in the literature, was found not to affect the spectral and self-aggregation behaviors of amphiphiles.

Pyrene Fluorescence Study. Fluorescence measurements, using pyrene as the fluorescent probe, were taken in a FluoroMax-4 spectrofluorometer from Horiba Scientific, using a 4 mL quartz cuvette with a 1 cm optical path. Excitation was done at 331.5 nm, and emissions were recorded in the 340−350 nm wavelength range. The slit widths for both excitation and emission were fixed at 0.4 nm. A 2 mg/mL solution of amphipathic species (copolymers and copolymer nanodiscs), dissolved in buffer (pH 7 at 25 °C) and 1 μM pyrene, was progressively diluted by removing 500 μL and adding 500 μL of a fresh pyrene-containing buffer. Thus, the pyrene concentration was constant through the dilution of the amphipathic species. The scan time was fixed at 0.8 s per scan. All measurements were thermostatically controlled at 25.0 ± 0.1 °C using a Quantum Northwest TC 1 temperature controller.[46] The ratio of the intensities of the fluorescence peaks I_1 and I_3 is plotted against the decimal logarithm of the concentration of the considered amphipathic species. Experimental data are shown in Figures 2−4, S1−S3, S5, Tables 1 and 2.

Table 1. Physicochemical Data of the Investigated SMA Copolymers[a]

copolymer	M_w (kDa)	x/y (molar ratio)	x_0 (mg/mL)	R^2
SMA-EA	∼2	∼1.3:1	0.23	0.992
SL25010 P	∼10	∼3:1	0.038	0.999
SL30010 P	∼7.5	∼2.3:1	0.26	0.998
SL40005 P	∼5	∼1.4:1	27	0.999

[a]Spanning a range of molecular weights from ∼2 to ∼10 kDa, each copolymer has comparable dispersity ($Đ = M_w/M_n > 2.5$) but different hydrophobicity−hydrophilicity ratios, as suggested from the styrene-to-maleic acid ratio. Additionally, SMA-EA shows a modified charge density because of its modification if compared to any SMA equivalent. The experimental curves I_1/I_3 vs log C shown in Figure 2a were fitted to a sigmoidal function. The c.m.c. values for each copolymer were obtained by calculating the flex (x_0) of each fitted curve and converted from a decimal logarithmic scale to a linear scale. The coefficient of determination, R^2, is also shown for each fitting. Experimental conditions are reported in the Methods section. Spectra and data are shown in Figures 2a, 3a, and S1.

Size Exclusion Chromatography (SEC). Copolymer−lipid nanodiscs were purified using a self-packed Sephadex 200 16/600 column operated on a GE Healthcare AKTA purifier. Samples were eluted at room temperature and at a buffer flow rate of 1 mL/min. The buffer used was 10 mM potassium phosphate buffer, pH 7 at 25 °C. The elution was monitored using a UV-detector at λ = 254 nm. Chromatograms are shown in Figure S4.

NMR Spectroscopy. Solution ^{1}H NMR experiments were performed using a 500 MHz Bruker Avance III HD NMR spectrometer. NMR samples were prepared according to the procedure described in the Copolymer−Lipid Nanodisc Preparation section but using 10 mM sodium phosphate buffer, pH 7.2, to avoid spectral interferences. All samples analyzed through NMR spectroscopy were lyophilized for 24 h before resuspension in 600 μL of 10 mM sodium cholate in D_2O, then transferred to 4 mm Norrell Sample Vault Series glass tubes, and placed in a commercial 5 mm triple-resonance ^{1}H/^{19}F/^{13}C Bruker round-coil TXITM 500 SB probe. ^{1}H NMR spectra were recorded by collecting 32 scans with a spectral

https://dx.doi.org/10.1021/acs.langmuir.0c03554
Langmuir 2021, 37, 3113−3121

Table 2. Copolymer–Lipid Nanodisc Data: Unpurified vs Purified[a]

	unpurified nanodiscs			unpurified nanodiscs			purified nanodiscs		
copolymer	x_0 (log C)	x_0(mg/mL)	R^2	x_0 (log[DMPC])	x_0 (mM)	R^2	x_0 (log[DMPC])	x_0 (mM)	R^2
SMA-EA	−2.12	7.59×10^{-3}	0.994	−1.95	1.12×10^{-2}	0.994	−1.60	2.51×10^{-2}	0.999
SL25010 P	−2.27	5.37×10^{-3}	0.998	−2.10	7.94×10^{-3}	0.998	−1.53	2.95×10^{-2}	0.998
SL30010 P	−2.50	3.16×10^{-3}	0.979	−2.33	4.68×10^{-3}	0.979	−1.55	2.82×10^{-2}	0.998
SL40005 P	−2.31	4.90×10^{-3}	0.999	−2.14	7.24×10^{-3}	0.999	−1.68	2.09×10^{-2}	0.999

[a]From left-to-right, the chart shows the data plotted respectively in Figures 2 and 4. The polymer-based nanodiscs were obtained by mixing the lipids and the copolymers in a 1:1 weight ratio, as detailed in the Methods section. Unpurified nanodiscs appear twice, as a function of the polymer concentration (C in mg/mL) and as a function of the DMPC concentration (mM). The "c.m.c.-like" values for each copolymer nanodisc were obtained by calculating the flex (x_0) of each fitted curve and converted from a decimal logarithmic scale to a linear scale. The coefficient of determination, R^2, is also shown for each fitting. Spectra and data are shown in Figures S1–S3 and S5.

width of 25 ppm. The ^{1}H transmitter frequency offset was set at 4.7 ppm. The experiments were performed at 35 °C to maximize the sharpness of lipid peaks and ensure a better integration. The concentration of each sample was detected using sodium cholate as an internal standard. ^{1}H NMR spectra and integration are shown in Figures S7–S11.

Atomic Force Microscopy (AFM) Coupled with Micro-Raman ***Spectroscopy.*** AFM measurements were done in alternate contact mode with a SiC tip of 2.8 N/m, using a Witec Alpha 300 RA. Images were acquired in 256 points by 256 lines, with maps 5 × 5 μm^2. Micro-Raman spectra were acquired using Witec Alpha 300 RA that employs a 532 nm laser operating at 20 mW. Two solutions of nanodiscs, 1 and 0.001 mg/mL, were drop-cast on a flat bare silicon substrate, cleaned with a 4% v/v hydrogen fluoride (HF) solution, and then dried at 30 °C. Raman experiments were performed on the same samples. The results are shown in Figures 4 and S6.

RESULTS AND DISCUSSION

In this study, we use a set of amphipathic copolymers to systematically investigate how the solution physicochemical properties of the copolymers can be associated with the features of copolymer–lipid nanodiscs to increase nanodiscs' performances and to assist the design of new copolymers. It is accepted that copolymer–lipid nanodisc solutions are stable under a wide range of conditions.[26,42,47] However, evidence suggests that despite the temporal stability, these nanoparticles show a high degree of dynamism as simplified in the scheme presented in Figure 1b.

It has been demonstrated that copolymer nanodiscs can exchange phospholipids,[48−50] but the exchange of copolymer chains cannot be neglected.[51] This phenomenon occurs either among nanodiscs due to collisions or among the polymer chains that are bound in the nanodiscs and those that are free in solution as micelles. In the latter, copolymer chains can be coiled or elongated as a consequence of changes in the parameters, such as pH, ionic strength, temperature, and pressure.[43,52] Copolymer micelles can be intrachain, interchain, or mixed. Additionally, the inevitable dispersity of any polymer sample can complicate the scenario.

The SMA-EA copolymer[36] is compared to a set of XIRAN commercially available SMA copolymer formulations.[53] Figure 1a shows the structural similarities among the copolymers, while Table 1 displays the technical properties of each formulation. Due to their amphipathic nature, SMA copolymers and their derivatives form self-assembled macromolecular aggregates. The c.m.c. is a crucial value to assess amphipathic molecules. Pyrene, a four-ring polycyclic aromatic hydrocarbon (PAH), is known to be a convenient fluorescent probe for determining the c.m.c. of amphipathic aggregates.[46,54] Pyrene is strongly hydrophobic and shows minimal solubility in water (~2 to 3 μM).[54] Therefore, it easily inserts in the hydrophobic

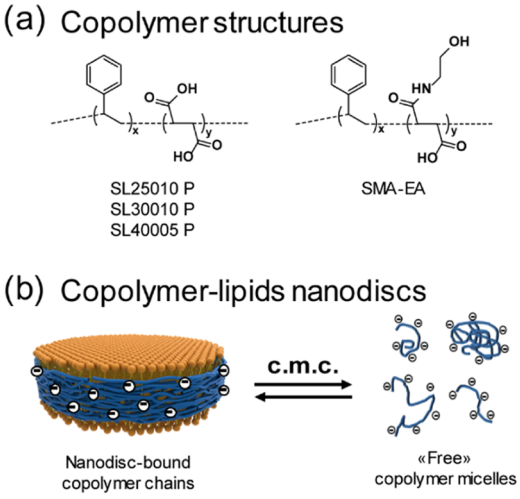

Figure 1. Chemical structures of SMA-based copolymers and copolymer–lipid nanodiscs. (a) Chemical structures of the copolymers used in this study. The chemical structures of XIRAN copolymers (SL25010 P, SL30010 P, and SL40005 P) provided by Polyscience are shown on the left and differ from each other in molecular weight and styrene-to-maleic acid (x/y) molar ratio. SMA-EA is a functionalized low-molecular-weight derivative of SMA with a reduced charge density.[36] More details are provided in Table 1. All structures are shown in their fully protonated form. (b) Simplified schematic representation of the chemical equilibrium between "nanodisc-bound" and "unbound/free-micellar" copolymer chains.

core of amphipathic micellelike aggregates and in the copolymer–lipid nanodiscs. Upon dilution, the micellar aggregate is destroyed, and pyrene molecules are directly exposed to water. This event, because of the solvent-dependent vibronic fine structure intensities shown by monomeric pyrene,[46,54] is profitably employed in fluorescence probe studies of amphipathic aggregates.

Figure 2 shows a selection of spectra that highlights the spectral changes of pyrene-containing solutions. When pyrene molecules are in the hydrophobic environment offered by copolymeric micellelike aggregates (Figure 2a) or in the copolymer–lipid nanodiscs (Figure 2b), pyrene fluorescent spectra are of low intensity. Similarities were observed among the investigated copolymers and the copolymer–lipid nanodiscs. The "shoulder" after 400 nm for the SL40005 P copolymer (green spectrum in Figure 2a) is due to scattering attributed to the high concentration used. The fluorescent spectrum of pyrene in the buffer solution (purple spectrum) simulates the infinite-dilution plateau or complete absence of amphipathic species. The crowding in hydrophobic environ-

https://dx.doi.org/10.1021/acs.langmuir.0c03554
Langmuir 2021, 37, 3113−3121

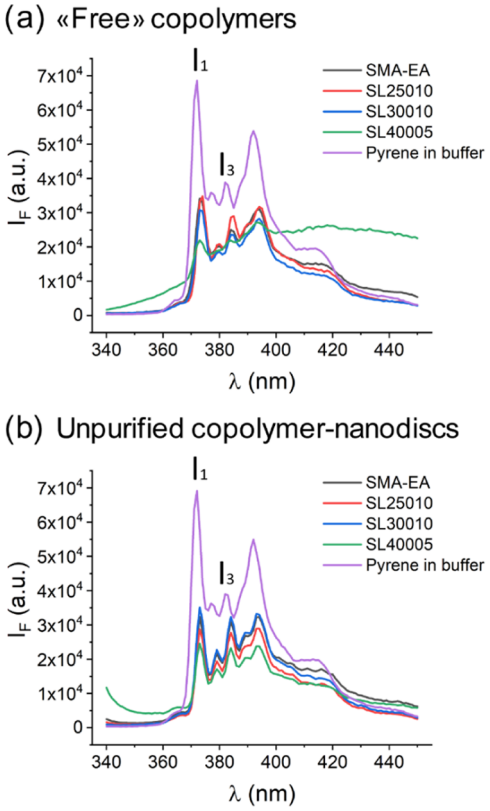

Figure 2. Pyrene fluorescence spectra of (a) "free" copolymers and (b) copolymer–lipid nanodiscs upon excitation at 331.5 nm. (a) Fluorescence spectra of pyrene in the presence of SMA-EA (black line), SL25010 P (red line), SL30010 P (blue line), or SL40005 (green line) copolymers free in solution and at the highest concentration used in this study. (b) Fluorescence spectra of pyrene in the presence of unpurified SMA-EA-based nanodiscs (black line), SL25010 P-based nanodiscs (red line), SL30010 P-based nanodiscs (blue line), or SL40005 P (green line) at the highest concentration used in this study. In purple, both (a) and (b) show the fluorescence spectrum of 1 μM pyrene, which can be associated with the most diluted sample or the "infinite-dilution sample". Each sample was prepared in 10 mM ammonium acetate buffer at pH 7 at 25 °C, spectra were recorded at 25 °C, and pyrene concentration was kept constant at 1 μM.

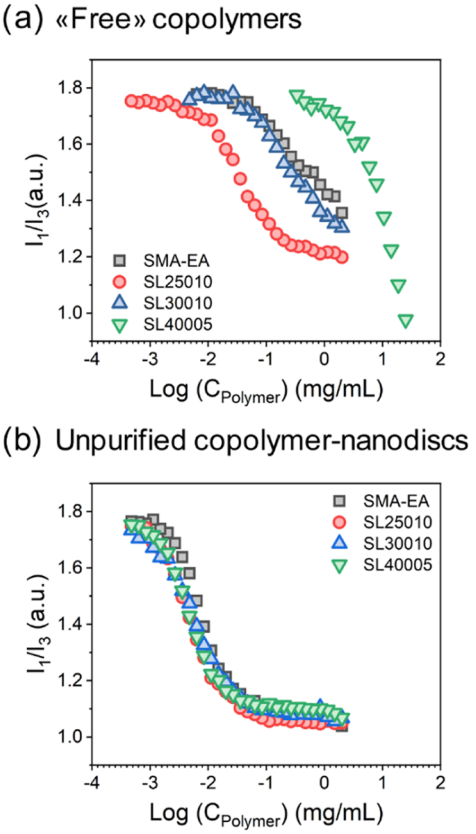

Figure 3. Copolymers show drastic changes in the presence of phospholipids. (a) Plots of the pyrene I_1/I_3 ratio against the decimal logarithm of the concentration of the copolymers in mg/mL. As expected from the physicochemical properties listed in Table 1, the polymer SL25010 P (circles in red) is the most hydrophobic, while SL40005 P (triangles in green) is the most hydrophilic. SMA-EA (black squares) and SL30010 P (blue triangles) show comparable responses. (b) Plots of the pyrene I_1/I_3 ratio against the concentration of copolymer–lipid nanodiscs in solution. The concentration is reported as a function of the decimal logarithm of the polymer concentration in mg/mL. Interestingly, when interacting with lipids, the differences observed in (a) become negligible among all of the copolymers. Both (a) and (b) show the average of three experiments obtained from independent samples. Each sample was prepared in 10 mM ammonium acetate buffer at pH 7 at 25 °C, spectra were recorded at 25 °C, and pyrene concentration was kept constant at 1 μM. Data, error bars, and fitting are reported in Figures S1 and S2.

ments justifies the quenching of pyrene fluorescence. By plotting the ratio of the intensities of the first and third fluorescence peaks, respectively, labeled as I_1 and I_3, against the decimal logarithm of the concentration, it is possible to obtain the c.m.c. values. Figure 3 shows the plot of the I_1/I_3 ratio for solutions of copolymers against the decimal logarithmic concentration of copolymers (Figure 3a) and unpurified copolymer–lipid nanodiscs (Figure 3b).

Results shown in Figure 3a are supported by the previous knowledge on the structure–property relationships[55] and agree with previously reported results[35] and the physicochemical properties summarized in Table 1. On the one hand, SL40005 P is the most hydrophilic formulation due to its relatively low molecular weight (M_w ~ 5 kDa), the low content of styrene repeating units (~1.4:1), and the associated high charge density. On the other hand, SL25010 P is the heaviest copolymer (M_w ~ 10 kDa) and the most hydrophobic formulation because of the 3:1 styrene-to-maleic acid molar ratio, which consequently results in a low charge density. For the same reasons, SL30010 P is placed in an intermediate position between these two cases (M_w ~ 7.5 kDa; 2.3:1).

Given the similarities among all of the formulations, AFM experiments were performed on SMA-EA/DMPC 1:1 (w/w) unpurified nanodiscs. Previous studies confirm that the adhesion among phosphocholine polar headgroups is responsible for the formation of stacked structures.[56] AFM images shown in Figure 4a,b were, respectively, obtained by drop-casting copolymer–lipid nanodisc solutions at a concentration above and below the copolymer's c.m.c.

The depth of DMPC bilayers is ~5 nm. Depth profiles shown in Figure 4a(I),(II) were obtained at 1 mg/mL. At such a high nanodisc concentration, stacks of DMPC nanodiscs are observed. For a 1000 times more diluted concentration, the depth profiles (III) and (IV) shown in Figure 4b confirm the existence of nanoparticles compatible with the height of DMPC bilayers and diameter compared to the size of SMA-

https://dx.doi.org/10.1021/acs.langmuir.0c03554
Langmuir 2021, 37, 3113−3121

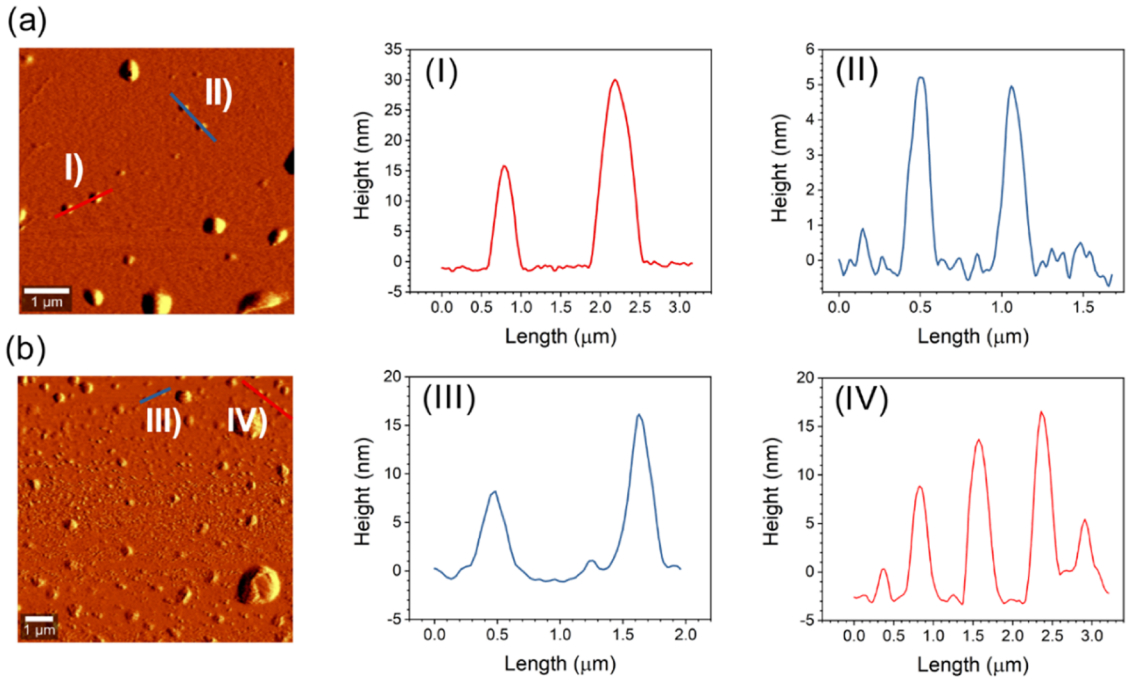

Figure 4. AFM images and depth profiles above and below the c.m.c. of the SMA-EA copolymer. (a) AFM image of a sample of 1 mg/mL DMPC/SMA-EA 1:1 w/w. (I) and (II) are the depth profiles indicated in (a). (b) AFM image of a sample of 0.001 mg/mL DMPC/SMA-EA 1:1 w/w. (III) and (IV) are the depth profiles indicated in (b). The Raman spectrum is shown in Figure S6.

EA−DMPC 1:1 w/w nanodiscs reported in the literature.[36] Raman vibrational experiments were used to confirm the presence of both copolymer and lipids in the 1 mg/mL sample used for AFM measurements (Figure S6). The process of membrane protein extraction occurs stepwise. After membrane dissolution, several steps of purification are involved before handling the final desired product.[7,14,57−59] Among the resulting materials, copolymer chains that are in equilibrium with the nanodisc-bound chains are discarded too. We speculate that this process, in addition to dilution, may alter the integrity of the nanodiscs as per the principle of chemical equilibrium. Size exclusion chromatography experiments were used herein to purify samples of copolymer−lipid nanodiscs. In fact, when copolymers were added to phospholipids, together with the formation of nanodiscs, a plethora of other micellar aggregates were formed. Chromatograms of model copolymer−lipid nanodiscs, reported in Figure S4, show two main peaks. The first is narrow and associated with the nanodiscs. The second is broad and usually related to the excess of micellar polymer chains. Copolymer micelles can display a plethora of morphologies,[60] and mixed unstructured copolymer chain−lipid aggregates cannot be excluded. This provides a variety of potential dynamic subunits for higher-level assemblies that could explain the breadth of the second chromatographic peak. Despite the physicochemical differences in the copolymers, after the purification step, copolymer−lipid nanodiscs behave similarly to the unpurified counterpart, as shown in Figure 3b. Figure 5 shows a comparison between samples of unpurified and purified lipid nanodiscs for each used copolymer formulation. A deeper analysis is presented in Table 2.

It is observable how the flex (x_0), associated with the nanodiscs' c.m.c., shifts toward higher concentration values. After purification, with the removal of the micellar aggregates in solution, SMA-EA nanodiscs shift by 2.2 times, while SL25010, SL30010, and SL40005 nanodiscs shift by 3.7, 6, and 2.9 times, respectively. This supports the existence of chemical equilibrium as schematically represented in Figure 1b. Data with error bars and fitting are presented in Figures S3 and S5.

CONCLUSIONS

In this study, we report the use of an analytic assay to assess the c.m.c. of SMA-based copolymers and to find connections among the c.m.c. and the integral stability of the nanodiscs intended as nanoparticles. The major findings of this study are as follows. (i) The c.m.c. of the SMA-EA copolymer, produced in our laboratory, is reported for the first time in comparison with some commercially available SMA copolymer formulations (XIRAN). (ii) The interaction with phospholipids drastically alters the copolymer's c.m.c. values. When in the form of nanodiscs, it is not possible to discern among pure copolymer's c.m.c. and pure phospholipid contributions, making it necessary to use a more generic concept such as the nanodisc c.m.c. (iii) Pieces of evidence suggest the existence of a chemical equilibrium among the free or "micellar" copolymer chains and the nanodisc-bound copolymer chains. Further investigations to evaluate the effect of the removal of free/micellar copolymers on the stability of nanodiscs (unpurified vs purified behavior) could be useful to fully characterize the properties of polymers and nanodiscs. We speculate that this phenomenon can be exploited to exchange belts in samples of copolymer−lipid nanodiscs. Indeed, a given formulation can be more successful in the extraction but not suitable with some biophysical or biochemical techniques. Additionally, a more inexpensive copolymer can be used to successfully extract and stabilize membrane proteins and then be substituted with tagged copolymers,[19,40,61,62] more expensive solution, optimizing costs and benefits.

https://dx.doi.org/10.1021/acs.langmuir.0c03554
Langmuir 2021, 37, 3113−3121

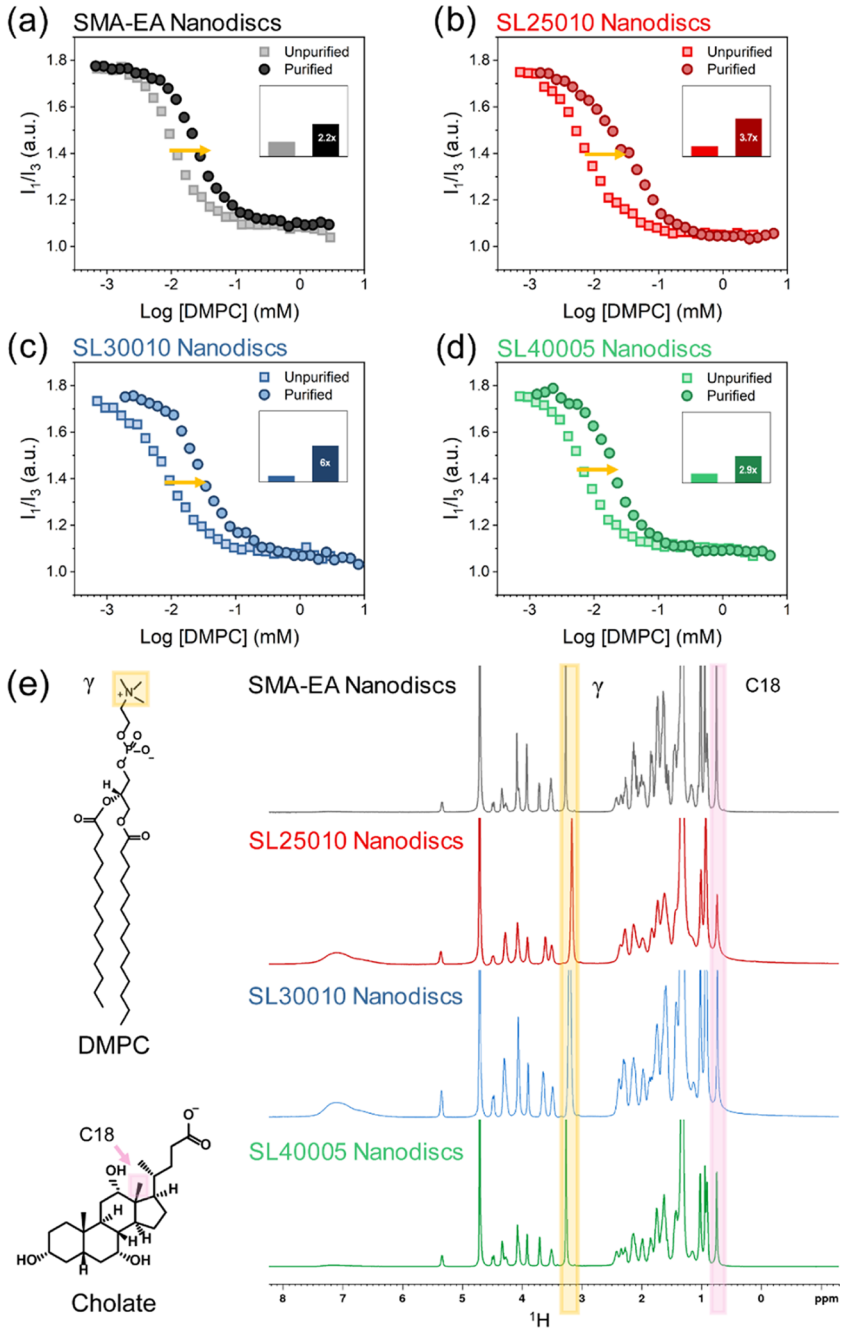

Figure 5. Comparison of the pyrene I_1/I_3 ratio against the concentration of unpurified (squares) and purified (circles) copolymer nanodiscs in solution. By purification through SEC, the removal of the micellar polymer not bound to the nanodisc edge causes a consistent horizontal shift for all of the copolymer formulations investigated, as reported in (a)−(d). The micellar polymer removed by SEC is either an excess or in chemical equilibrium among the states nanodisc-bound and unbound/free-micellar in solution. The insets in (a)−(d) show the shift in the middle flex point of the plots I_1/I_3 vs log[DMPC] for unpurified and purified nanodisc samples as indicated by the horizontal arrows. Each sample was prepared in 10 mM ammonium acetate buffer at pH 7 at 25 °C, spectra were recorded at 25 °C, and pyrene concentration was kept constant at 1 μM. Data, error bars, and fitting are reported in Figures S3 and S5. The concentration of SEC-purified copolymer−lipid nanodiscs was assessed through ^{1}H NMR using sodium cholate as an internal standard as described in the Methods section and shown in (e). Detailed spectra are provided in Figures S7−S11.

■ ASSOCIATED CONTENT

Supporting Information

The Supporting Information is available free of charge at https://pubs.acs.org/doi/10.1021/acs.langmuir.0c03554.

Pyrene fluorescence essays on copolymers, unpurified copolymer−lipid nanodiscs, and purified copolymer−lipid nanodiscs; Raman spectrum of nanodiscs; size exclusion chromatograms; and ^{1}H NMR spectra of copolymer−lipid nanodiscs (PDF)

■ AUTHOR INFORMATION

Corresponding Authors

Giacomo M. Di Mauro − *Department of Chemistry, University of Michigan, Ann Arbor, Michigan 48109-1055,*

https://dx.doi.org/10.1021/acs.langmuir.0c03554
Langmuir 2021, 37, 3113−3121

United States; orcid.org/0000-0002-6990-1304; Email: gdimauro@umich.edu

Ayyalusamy Ramamoorthy − *Department of Chemistry and Biophysics and Chemistry Department, Macromolecular Science and Engineering, and Biomedical Engineering, University of Michigan, Ann Arbor, Michigan 48109-1055, United States;* orcid.org/0000-0003-1964-1900; Email: ramamoor@umich.edu

Authors

Carmelo La Rosa − *Department of Chemistry, University of Catania, Catania 95125, Italy;* orcid.org/0000-0002-7123-5347

Marcello Condorelli − *Department of Chemistry, University of Catania, Catania 95125, Italy*

Complete contact information is available at: https://pubs.acs.org/10.1021/acs.langmuir.0c03554

Author Contributions

G.M.D.M. and A.R. designed the project and interpreted the results. G.M.D.M carried out the experiments, processed the data, and drafted the manuscript in discussion with A.R. C.L.R. and M.C. performed AFM experiments and analyzed the results. All authors reviewed, edited the final draft, and have given approval to the final version of the manuscript. A.R. supervised and directed the project.

Funding

This research was supported by the National Institute of Health (R35GM139573 to A.R.). Research in the CLR laboratory was supported by the University of Catania Departmental Project 2017−2020 (Progetto di Dipartimento 2017−2020). Experiments at the Bio-Nanotech Research and Innovation Tower (BRIT), University of Catania, Italy, were financed by the Italian Ministry of Education, University and Research (Ministero per l'istruzione, l'Universitá e la Ricerca, MIUR). CLR and MC thank G. F. Indelli (BRIT) for technical support.

Notes

The authors declare no competing financial interest.

■ ACKNOWLEDGMENTS

The authors thank Polyscience (Geleen, Netherlands) for gifting the formulations of XIRAN SL25010 P, SL30010 P, and SL40005 P and Dr. Thirupathi Ravula for providing the SMA-EA copolymer.

■ REFERENCES

(1) Overington, J. P.; Al-Lazikani, B.; Hopkins, A. L. How Many Drug Targets Are There? *Nat. Rev. Drug Discovery* **2006**, *5*, 993−996.

(2) Yeagle, P. L. Non-Covalent Binding of Membrane Lipids to Membrane Proteins. *Biochim. Biophys. Acta, Biomembr.* **2014**, *1838*, 1548−1559.

(3) Sun, C.; Benlekbir, S.; Venkatakrishnan, P.; Wang, Y.; Hong, S.; Hosler, J.; Tajkhorshid, E.; Rubinstein, J. L.; Gennis, R. B. Structure of the Alternative Complex III in a Supercomplex with Cytochrome Oxidase. *Nature* **2018**, *557*, 123−126.

(4) Hagn, F.; Etzkorn, M.; Raschle, T.; Wagner, G. Optimized Phospholipid Bilayer Nanodiscs Facilitate High-Resolution Structure Determination of Membrane Proteins. *J. Am. Chem. Soc.* **2013**, *135*, 1919−1925.

(5) Simon, K. S.; Pollock, N. L.; Lee, S. C. Membrane Protein Nanoparticles: The Shape of Things to Come. *Biochem. Soc. Trans.* **2018**, *46*, 1495−1504.

(6) Parmar, M. J.; Lousa, C. D. M.; Muench, S. P.; Goldman, A.; Postis, V. L. G. Artificial Membranes for Membrane Protein Purification, Functionality and Structure Studies. *Biochem. Soc. Trans.* **2016**, *44*, 877−882.

(7) Lee, S. C.; Knowles, T. J.; Postis, V. L. G.; Jamshad, M.; Parslow, R. A.; Lin, Y.; Goldman, A.; Sridhar, P.; Overduin, M.; Muench, S. P.; et al. A Method for Detergent-Free Isolation of Membrane Proteins in Their Local Lipid Environment. *Nat. Protoc.* **2016**, *11*, 1149−1162.

(8) Knowles, T. J.; Finka, R.; Smith, C.; Lin, Y.-P.; Dafforn, T.; Overduin, M. Membrane Proteins Solubilized Intact in Lipid Containing Nanoparticles Bounded by Styrene Maleic Acid Copolymer. *J. Am. Chem. Soc.* **2009**, *131*, 7484−7485.

(9) Rajesh, S.; Knowles, T.; Overduin, M. Production of Membrane Proteins without Cells or Detergents. *New Biotechnol.* **2011**, *28*, 250−254.

(10) Jamshad, M.; Lin, Y.-P.; Knowles, T. J.; Parslow, R. A.; Harris, C.; Wheatley, M.; Poyner, D. R.; Bill, R. M.; Thomas, O. R. T.; Overduin, M.; et al. Surfactant-Free Purification of Membrane Proteins with Intact Native Membrane Environment. *Biochem. Soc. Trans.* **2011**, *39*, 813−818.

(11) Hardin, N. Z.; Ravula, T.; Mauro, G. D.; Ramamoorthy, A. Hydrophobic Functionalization of Polyacrylic Acid as a Versatile Platform for the Development of Polymer Lipid Nanodisks. *Small* **2019**, *15*, No. 1804813.

(12) Yasuhara, K.; Arakida, J.; Ravula, T.; Ramadugu, S. K.; Sahoo, B.; Kikuchi, J.-I.; Ramamoorthy, A. Spontaneous Lipid Nanodisc Fomation by Amphiphilic Polymethacrylate Copolymers. *J. Am. Chem. Soc.* **2017**, *139*, 18657−18663.

(13) Ravula, T.; Hardin, N. Z.; Bai, J.; Im, S. C.; Waskell, L.; Ramamoorthy, A. Effect of Polymer Charge on Functional Reconstitution of Membrane Proteins in Polymer Nanodiscs. *Chem. Commun.* **2018**, *54*, 9615−9618.

(14) Dörr, J. M.; Scheidelaar, S.; Koorengevel, M. C.; Dominguez, J. J.; Schäfer, M.; van Walree, C. A.; Killian, J. A. The Styrene−Maleic Acid Copolymer: A Versatile Tool in Membrane Research. *Eur. Biophys. J.* **2016**, *45*, 3−21.

(15) Ravula, T.; Hardin, N. Z.; Di Mauro, G. M.; Ramamoorthy, A. Styrene Maleic Acid Derivates to Enhance the Applications of Bio-Inspired Polymer Based Lipid-Nanodiscs. *Eur. Polym. J.* **2018**, *108*, 597−602.

(16) Overduin, M.; Klumperman, B. Advancing Membrane Biology with Poly(Styrene-Co-Maleic Acid)-Based Native Nanodiscs. *Eur. Polym. J.* **2019**, *110*, 63−68.

(17) Hall, S. C. L.; Tognoloni, C.; Price, G. J.; Klumperman, B.; Edler, K. J.; Dafforn, T. R.; Arnold, T. Influence of Poly(Styrene-Co-Maleic Acid) Copolymer Structure on the Properties and Self-Assembly of SMALP Nanodiscs. *Biomacromolecules* **2018**, *19*, 761−772.

(18) Oluwole, A. O.; Danielczak, B.; Meister, A.; Babalola, J. O.; Vargas, C.; Keller, S. Solubilization of Membrane Proteins into Functional Lipid-Bilayer Nanodiscs Using a Diisobutylene/Maleic Acid Copolymer. *Angew. Chem., Int. Ed.* **2017**, *56*, 1919−1924.

(19) Lindhoud, S.; Carvalho, V.; Pronk, J. W.; Aubin-Tam, M. E. SMA-SH: Modified Styrene-Maleic Acid Copolymer for Functionalization of Lipid Nanodiscs. *Biomacromolecules* **2016**, *17*, 1516−1522.

(20) Brady, N. G.; Qian, S.; Bruce, B. D. Analysis of Styrene Maleic Acid Alternating Copolymer Supramolecular Assemblies in Solution by Small Angle X-Ray Scattering. *Eur. Polym. J.* **2019**, *111*, 178−184.

(21) Morrison, K. A.; Akram, A.; Mathews, A.; Khan, Z. A.; Patel, J. H.; Zhou, C.; Hardy, D. J.; Moore-Kelly, C.; Patel, R.; Odiba, V.; et al. Membrane Protein Extraction and Purification Using Styrene-Maleic Acid (SMA) Copolymer: Effect of Variations in Polymer Structure. *Biochem. J.* **2016**, *473*, 4349−4360.

(22) Gulamhussein, A. A.; Meah, D.; Soja, D. D.; Fenner, S.; Saidani, Z.; Akram, A.; Lallie, S.; Mathews, A.; Painter, C.; Liddar, M. K.; et al. Examining the Stability of Membrane Proteins within SMALPs. *Eur. Polym. J.* **2019**, *112*, 120−125.

(23) Krishnarjuna, B.; Ravula, T.; Ramamoorthy, A. Detergent-Free Extraction, Reconstitution and Characterization of Membrane-

Anchored Cytochrome-B5 in Native Lipids. *Chem. Commun.* **2020**, *56*, 6511−6514.
(24) Overduin, M.; Esmaili, M. Memtein: The Fundamental Unit of Membrane-Protein Structure and Function. *Chem. Phys. Lipids* **2019**, *218*, 73−84.
(25) Reading, E.; Hall, Z.; Martens, C.; Haghighi, T.; Findlay, H.; Ahdash, Z.; Politis, A.; Booth, P. J. Interrogating Membrane Protein Conformational Dynamics within Native Lipid Compositions. *Angew. Chem., Int. Ed.* **2017**, *56*, 15654−15657.
(26) Simon, K. S.; Pollock, N. L.; Lee, S. C. Membrane Protein Nanoparticles: The Shape of Things to Come. *Biochem. Soc. Trans.* **2018**, *46*, 1495−1504.
(27) Orwick-Rydmark, M.; Lovett, J. E.; Graziadei, A.; Lindholm, L.; Hicks, M. R.; Watts, A. Detergent-Free Incorporation of a Seven-Transmembrane Receptor Protein into Nanosized Bilayer Lipodisq Particles for Functional and Biophysical Studies. *Nano Lett.* **2012**, *12*, 4687−4692.
(28) Cuevas Arenas, R.; Klingler, J.; Vargas, C.; Keller, S. Influence of Lipid Bilayer Properties on Nanodisc Formation Mediated by Styrene/Maleic Acid Copolymers. *Nanoscale* **2016**, *8*, 15016−15026.
(29) Stroud, Z.; Hall, S. C. L.; Dafforn, T. R. Purification of Membrane Proteins Free from Conventional Detergents: SMA, New Polymers, New Opportunities and New Insights. *Methods* **2018**, *147*, 106−117.
(30) Huang, J.; Turner, S. R. Recent Advances in Alternating Copolymers: The Synthesis, Modification, and Applications of Precision Polymers. *Polymer* **2017**, *116*, 572−586.
(31) Klumperman, B. Mechanistic Considerations on Styrene-Maleic Anhydride Copolymerization Reactions. *Polym. Chem.* **2010**, *1*, 558−562.
(32) Lessard, B.; Marić, M. One-Step Poly(Styrene-Alt-Maleic Anhydride)-Block-Poly(Styrene) Copolymers with Highly Alternating Styrene/Maleic Anhydride Sequences Are Possible by Nitroxide-Mediated Polymerization. *Macromolecules* **2010**, *43*, 879−885.
(33) Craig, A. F.; Clark, E. E.; Sahu, I. D.; Zhang, R.; Frantz, N. D.; Al-Abdul-Wahid, M. S.; Dabney-Smith, C.; Konkolewicz, D.; Lorigan, G. A. Tuning the Size of Styrene-Maleic Acid Copolymer-Lipid Nanoparticles (SMALPs) Using RAFT Polymerization for Biophysical Studies. *Biochim. Biophys. Acta, Biomembr.* **2016**, *1858*, 2931−2939.
(34) Smith, A. A. A.; Autzen, H. E.; Laursen, T.; Wu, V.; Yen, M.; Hall, A.; Hansen, S. D.; Cheng, Y.; Xu, T. Controlling Styrene Maleic Acid Lipid Particles through RAFT. *Biomacromolecules* **2017**, *18*, 3706−3713.
(35) Scheidelaar, S.; Koorengevel, M. C.; van Walree, C. A.; Dominguez, J. J.; Dörr, J. M.; Killian, J. A. Effect of Polymer Composition and PH on Membrane Solubilization by Styrene-Maleic Acid Copolymers. *Biophys. J.* **2016**, *111*, 1974−1986.
(36) Ravula, T.; Ramadugu, S. K.; Di Mauro, G. M.; Ramamoorthy, A. Bioinspired, Size-Tunable Self-Assembly of Polymer−Lipid Bilayer Nanodiscs. *Angew. Chem., Int. Ed.* **2017**, *56*, 11466−11470.
(37) Ravula, T.; Hardin, N. Z.; Ramadugu, S. K.; Ramamoorthy, A. PH Tunable and Divalent Metal Ion Tolerant Polymer Lipid Nanodiscs. *Langmuir* **2017**, *33*, 10655−10662.
(38) Ravula, T.; Hardin, N. Z.; Ramadugu, S. K.; Cox, S. J.; Ramamoorthy, A. Formation of PH-Resistant Monodispersed Polymer-Lipid Nanodiscs. *Angew. Chem., Int. Ed.* **2018**, *57*, 1342−1345.
(39) Harding, B. D.; Dixit, G.; Burridge, K. M.; Sahu, I. D.; Dabney-Smith, C.; Edelmann, R. E.; Konkolewicz, D.; Lorigan, G. A. Characterizing the Structure of Styrene-Maleic Acid Copolymer-Lipid Nanoparticles (SMALPs) Using RAFT Polymerization for Membrane Protein Spectroscopic Studies. *Chem. Phys. Lipids* **2019**, *218*, 65−72.
(40) Di Mauro, G. M.; Hardin, N. Z.; Ramamoorthy, A. Lipid-Nanodiscs Formed by Paramagnetic Metal Chelated Polymer for Fast NMR Data Acquisition. *Biochim. Biophys. Acta, Biomembr.* **2020**, *1862*, No. 183332.
(41) Ravula, T.; Hardin, N. Z.; Ramamoorthy, A. Polymer Nanodiscs: Advantages and Limitations. *Chem. Phys. Lipids* **2019**, *219*, 45−49.
(42) Dörr, J. M.; Koorengevel, M. C.; Schäfer, M.; Prokofyev, A. V.; Scheidelaar, S.; van der Cruijsen, E. A. W.; Dafforn, T. R.; Baldus, M.; Killian, J. A. Detergent-Free Isolation, Characterization, and Functional Reconstitution of a Tetrameric K+ Channel: The Power of Native Nanodiscs. *Proc. Natl. Acad. Sci. U.S.A.* **2014**, *111*, 18607−18612.
(43) Owen, S. C.; Chan, D. P. Y.; Shoichet, M. S. Polymeric Micelle Stability. *Nano Today* **2012**, *7*, 53−65.
(44) Stetsenko, A.; Guskov, A. An Overview of the Top Ten Detergents Used for Membrane Protein Crystallization. *Crystals* **2017**, *7*, 197.
(45) Mukerjee, P.; Mysels, K. J. *Critical Micelle Concentrations of Aqueous Surfactant Systems*; National Bureau of Standards, Washington D.C., 1971.
(46) Ray, G. B.; Chakraborty, I.; Moulik, S. P. Pyrene Absorption Can Be a Convenient Method for Probing Critical Micellar Concentration (Cmc) and Indexing Micellar Polarity. *J. Colloid Interface Sci.* **2006**, *294*, 248−254.
(47) Gulati, S.; Jamshad, M.; Knowles, T. J.; Morrison, K. A.; Downing, R.; Cant, N.; Collins, R.; Koenderink, J. B.; Ford, R. C.; Overduin, M.; et al. Detergent-Free Purification of ABC (ATP-Binding-Cassette) Transporters. *Biochem. J.* **2014**, *461*, 269−278.
(48) Danielczak, B.; Keller, S. Lipid Exchange among Polymer-Encapsulated Nanodiscs by Time-Resolved Förster Resonance Energy Transfer. *Methods* **2020**, *180*, 27−34.
(49) Oluwole, A. O.; Klingler, J.; Danielczak, B.; Babalola, J. O.; Vargas, C.; Pabst, G.; Keller, S. Formation of Lipid-Bilayer Nanodiscs by Diisobutylene/Maleic Acid (DIBMA) Copolymer. *Langmuir* **2017**, *33*, 14378−14388.
(50) Hazell, G.; Arnold, T.; Barker, R. D.; Clifton, L. A.; Steinke, N. J.; Tognoloni, C.; Edler, K. J. Evidence of Lipid Exchange in Styrene Maleic Acid Lipid Particle (SMALP) Nanodisc Systems. *Langmuir* **2016**, *32*, 11845−11853.
(51) Schmidt, V.; Sturgis, J. N. Modifying Styrene-Maleic Acid Co-Polymer for Studying Lipid Nanodiscs. *Biochim. Biophys. Acta, Biomembr* **2018**, *1860*, 777−783.
(52) Qazi, M. J.; Schlegel, S. J.; Backus, E. H. G.; Bonn, M.; Bonn, D.; Shahidzadeh, N. Dynamic Surface Tension of Surfactants in the Presence of High Salt Concentrations. *Langmuir* **2020**, *36*, 7956−7964.
(53) Polyscience. Technical Datasheet https://www.polyscience.eu/smalp/technical-datasheet/ (accessed May 20, 2020).
(54) Kalyanasundaram, K.; Thomas, J. K. Solvent-Dependent Fluorescence of Pyrene-3-Carboxaldehyde and Its Applications in the Estimation of Polarity at Micelle-Water Interfaces. *J. Phys. Chem. A* **1977**, *81*, 2176−2180.
(55) Murphy, P. M. Teaching Structure-Property Relationships: Investigating Molecular Structure and Boiling Point. *J. Chem. Educ.* **2007**, *84*, 97−101.
(56) Brechling, A.; Sundermann, M.; Kleineberg, U.; Heinzmann, U. Characterization of DMPC Bilayers and Multilamellar Islands on Hydrophobic Self-Assembled Monolayers of ODS/Si(100) and Mixed ODS-DDS/Si(100). *Thin Solid Films* **2003**, *433*, 281−286.
(57) Postis, V.; Rawson, S.; Mitchell, J. K.; Lee, S. C.; Parslow, R. A.; Dafforn, T. R.; Baldwin, S. A.; Muench, S. P. The Use of SMALPs as a Novel Membrane Protein Scaffold for Structure Study by Negative Stain Electron Microscopy. *Biochim. Biophys. Acta, Biomembr.* **2015**, *1848*, 496−501.
(58) Parmar, M.; Rawson, S.; Scarff, C. A.; Goldman, A.; Dafforn, T. R.; Muench, S. P.; Postis, V. L. G. Using a SMALP Platform to Determine a Sub-Nm Single Particle Cryo-EM Membrane Protein Structure. *Biochim. Biophys. Acta, Biomembr.* **2018**, *1860*, 378−383.
(59) Kantola, A. M.; Lantto, P.; Heinmaa, I.; Vaara, J.; Jokisaari, J. Direct Magnetic-Field Dependence of NMR Chemical Shift. *Phys. Chem. Chem. Phys.* **2020**, *22*, 8485−8490.

https://dx.doi.org/10.1021/acs.langmuir.0c03554
Langmuir 2021, 37, 3113−3121

(60) Lu, Y.; Lin, J.; Wang, L.; Zhang, L.; Cai, C. Self-Assembly of Copolymer Micelles: Higher-Level Assembly for Constructing Hierarchical Structure. *Chem. Rev.* **2020**, *120*, 4111−4140.
(61) Hardin, N. Z.; Kocman, V.; Di Mauro, G. M.; Ravula, T.; Ramamoorthy, A. Metal-Chelated Polymer Nanodiscs for NMR Studies. *Angew. Chem., Int. Ed.* **2019**, *58*, 17246−17250.
(62) Kocman, V.; Di Mauro, G. M.; Veglia, G.; Ramamoorthy, A. Use of Paramagnetic Systems to Speed-up NMR Data Acquisition and for Structural and Dynamic Studies. *Solid State Nucl. Magn. Reson.* **2019**, *102*, 36−46.

https://dx.doi.org/10.1021/acs.langmuir.0c03554
Langmuir 2021, 37, 3113−3121